

Cite this: *Chem. Sci.*, 2023, 14, 14262

All publication charges for this article have been paid for by the Royal Society of Chemistry

An orbitally adapted push–pull template for N₂ activation and reduction to diazene-diide†

David Specklin, Marie-Christine Boegli, Anaïs Coffinet, Léon Escomel, Laure Vendier, Mary Grellier and Antoine Simonneau *

A Lewis superacidic bis(borane) C₆F₄{B(C₆F₅)₂}₂ was reacted with tungsten N₂-complexes [W(N₂)₂(R₂PCH₂CH₂PR₂)₂] (R = Ph or Et), affording zwitterionic boryldiazenido W(II) complexes *trans*-[W(L)(R₂PCH₂CH₂PR₂)₂(N₂{B(C₆F₅)₂(C₆F₄B(C₆F₅)₃))}] (L = ∅, N₂ or THF). These compounds feature only one N–B linkage of the covalent type, as a result of intramolecular boron-to-boron C₆F₅ transfer. Complex *trans*-[W(THF)(Et₂PCH₂CH₂PEt₂)₂(N₂{B(C₆F₅)₂C₆F₄B(C₆F₅)₃})] (5) was shown to split H₂, leading to a seven-coordinate complex [W(H)₂(Et₂PCH₂CH₂PEt₂)₂(N₂{B(C₆F₅)₂C₆F₄})] (7). Interestingly, hydride storage at the metal triggers backward C₆F₅ transfer. This reverts the bis(boron) moiety to its bis(borane) state, now doubly binding the distal N, with structural parameters and DFT computations pointing to dative N→B bonding. By comparison with an N₂ complex [W(H)₂(Et₂PCH₂CH₂PEt₂)₂(N₂{B(C₆F₅)₃})] (10) differing only in the Lewis acid (LA), namely B(C₆F₅)₃, coordinated to the distal N, we demonstrate that two-fold LA coordination imparts strong N₂ activation up to the diazene-diide (N₂²⁻) state. To the best of our knowledge, this is the first example of a neutral LA coordination that induces reduction of N₂.

Received 21st August 2023
Accepted 19th November 2023

DOI: 10.1039/d3sc04390h

rsc.li/chemical-science

Introduction

Dinitrogen activation by transition-metals as a means to transform this inert molecule under mild conditions has attracted the interest of chemists for almost 60 years.¹ Over the last five decades, dinitrogen complexes of the d-,¹ f-² and recently s-³ and p-⁴ block elements have been described in the literature, exhibiting a wealth of coordination modes, oxidation states and reactivity for the N₂ ligand. Some have shown potential as greener alternatives⁵ to the energy- and fossil fuel-intensive Haber–Bosch process,⁶ or for the synthesis of value-added (organo)nitrogen compounds.⁷ They can serve as models of the nitrogen-fixing enzymes nitrogenases, that feature an organometallic FeM (M = Mo, V or Fe) cofactor that can bind the diatomic molecule.⁸ Interaction of dinitrogen with a transition metal is well described by the Chatt–Dewar–Duncanson model:⁹ the metal centre “pushes” its d-electrons into the antibonding orbitals of N₂. High activation may ultimately be reached in dinuclear edifices through “push–push” activation.^{1b,10} “Push–pull” activation of dinitrogen¹¹ remains less explored. It consists of enhancing the polarization of dinitrogen when coordinated to a metal centre through non-covalent

interaction with an electron-deficient species,¹² mimicking to a certain extent the effect of secondary-sphere H-bonding between N₂ and the multiple acidic functions of nitrogenases' active site.^{12f,i,13,14} Several groups have evidenced that a single non-covalent interaction of a neutral transition-metal^{12a} or main group^{12b–g,j} Lewis acid (LA), an alkali^{12f,h} or Au(I)⁺ cation^{12j} or a weak acid¹²ⁱ (neutral or charged) leads to enhanced activation of N₂ thanks to augmented charge transfer (Fig. 1). A parallel between push–pull activation and the chemistry of frustrated Lewis pairs (FLPs)¹⁵ can be drawn, since the reactivity thereof resides in the synergistic action of a strong LA *pulling* electron density and a bulky Lewis base *pushing* its electron pair into antibonding orbitals of a substrate to activate. The chemistry of FLP still lacks a genuine N₂ capture example,¹⁶ but the Stephan group has proposed the B(C₆F₅)₃ adduct of diphenyldiazomethane as a model thereof (Fig. 1).^{17,18} The above-mentioned body of work thus provides clues of what to expect from push–pull or FLP-related N₂ activation in terms of structure, whereas the higher polarization of the N₂ unit in these compounds may ultimately lead to the discovery of new reactivity.^{12f,19} Besides, the N≡N→LA linkage may show FLP-type reactivity, such as Si–H bond heterolytic splitting, resulting in N₂ silylation.^{12g,20} Of note, the analogous reaction employing H₂ for N–H bond formation²¹ is yet to be achieved and is challenged by the propensity of H₂ to easily substitute N₂.²² Alternatively, [R₃XH]⁺[R'₃BH][−] (X = N or P) ion pairs delivered by FLP H₂ splitting²³ have been employed to protonate N₂.^{24,25}

Main-group Lewis acids interact with a molecular orbital of an N₂ complex that mixes a filled metal's d orbital and a π*

LCC-CNRS, Université de Toulouse, CNRS, UPS, 205 route de Narbonne, BP44099, F-31077 Toulouse Cedex 4, France. E-mail: antoine.simonneau@lcc-toulouse.fr

† Electronic supplementary information (ESI) available: Synthetic protocols, spectroscopic characterization, DFT computations, and CIF files. CCDC 2115061, 2115062, 2115063, 2115066 and 2285830. For ESI and crystallographic data in CIF or other electronic format see DOI: <https://doi.org/10.1039/d3sc04390h>

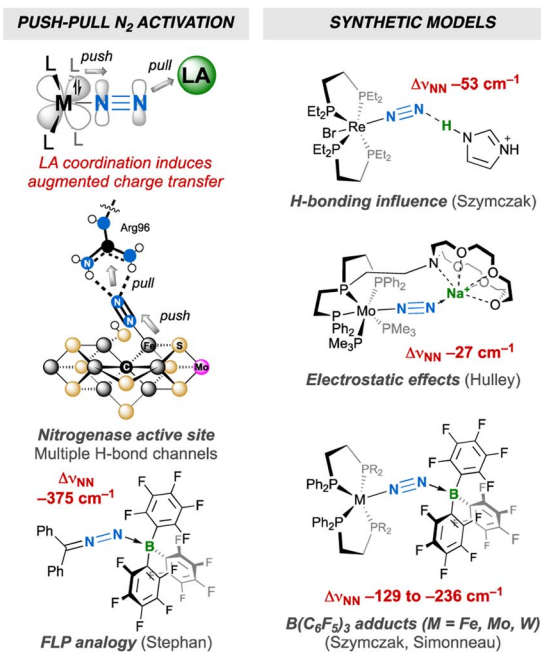


Fig. 1 N₂ push-pull activation: bioinorganic relevance, FLP analogy and synthetic models.

orbital of N₂.^{12fj,26} To the best of our knowledge, the two-fold coordination of a neutral LA to the distal N was never reported,^{27,28} although it would be interesting to judge how far the resulting push-pull effect affects the N₂ unit when compared to two-fold protonation^{24a,29} or functionalisation,³⁰ without being altered by the association of the conjugated base or leaving group with the metal that generally takes place in the two former cases. Such an achievement would also complement previous studies aimed at measuring the push-pull influence of monotopic LAs,¹² showing how multiple electron-deficient centres (as found in nitrogenases' active sites) may synergistically enhance N₂ activation. To this end, we have explored the coordination of a strongly electrophilic bis(borane) to a terminal N₂ complex (Fig. 1) and endeavour to compare the push-pull effect with the one induced by B(C₆F₅)₃. We hoped that the two empty p orbitals of the tethered B atoms would spatially match with the two lobes of the distal N's p orbital. Such an "orbitally adapted" push-pull template should result in high N₂ activation and polarisation as a result of greater stabilization of the d+π* frontier orbital (Fig. 2). In this article, we show that particular conditions should be met to observe two-

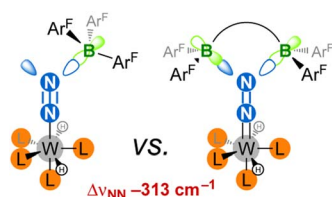
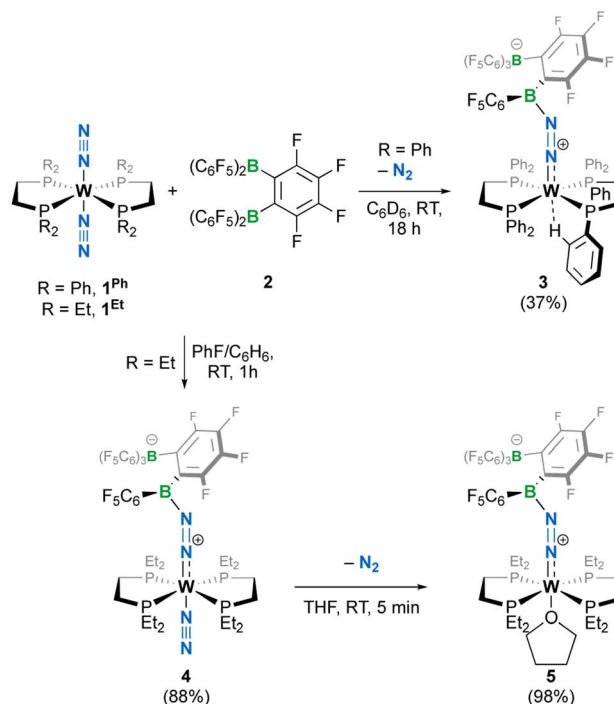


Fig. 2 This work: achievement of two-fold LA coordination on an N₂ ligand results in an extreme push-pull effect. Ar^F = C₆F₅.

fold coordination of the bis(borane). Indeed, hydride storage through H₂ oxidative addition at the metal-N₂ complex was key to achieve this goal, allowing us to discover that LA adducts of group 6 N₂ complexes may react with H₂ without N₂ loss (but not through FLP-type splitting). It is shown that two-fold LA coordination exerts a very strong influence on the diatomic molecule, and comparison of structural, spectroscopic and computational data supports its activation up to the 2-e⁻ reduced state.

Results and discussion

When we reacted equimolar amounts of the dinitrogen complexes [W{R₂P(CH₂)₂PR₂}₂(N₂)₂] (**1**^R with R = Ph or Et, Ph₂P(CH₂)₂PPh₂ = dppe and Et₂P(CH₂)₂PEt₂ = depe) with the Lewis superacidic³¹ bis(borane) C₆F₄-1,2-B(C₆F₅)₂ (**2**) reported by the Piers group,³² the rapid crystallization at room temperature of a new species [W(dppe)₂(N₂{B(C₆F₅)₂C₆F₄B(C₆F₅)₃})] **3** in moderate yield was observed (Scheme 1), whereas a depe analogue *trans*-[W(N₂)(depe)₂(N₂{B(C₆F₅)₂C₆F₄B(C₆F₅)₃})] **4** was obtained in high yield from a PhF/C₆H₆ mixture. Complexes **3** and **4** were found to be poorly soluble in toluene-*d*₈ or C₆D₆ and decomposed readily in CD₂Cl₂ or PhCl-*d*₅. When dissolved in THF-*d*₈, complex **3** converted immediately to a mixture of compounds whose identification was made difficult due to rapid polymerization of the medium. In the same solvent, **4** cleanly turns to a THF complex *trans*-[W(THF)(depe)₂(N₂{B(C₆F₅)₂C₆F₄B(C₆F₅)₃})] (**5**) after N₂ substitution, as evidenced by visible gas evolution. The latter could be isolated in high yield after removal of solvent under vacuum. Generation of **5** in a 1 : 1



Scheme 1 Syntheses of complexes **3**–**5**; isolated yields in parentheses.

reaction of **2** and **1^{Et}** in THF was not optimal as THF polymerization occurred upon solvation of the reactants. Complex **5** has been characterized in solution by ^1H , ^{31}P , ^{19}F and ^{11}B NMR spectroscopy. The ^1H and ^{31}P NMR were diagnostic of two pairs of inequivalent phosphine ligands with two pseudo-singlets in $^{31}\text{P}\{^1\text{H}\}$ NMR at 38.6 and 33.8 ppm, with $^2J_{\text{PP}}$ inferred by 2D experiments but too weak (<1 Hz) to be resolved (Fig. S5†). In ^{11}B NMR (Fig. S6†), only a well resolved borate resonance was observed as a singlet at -15.05 ppm, indicating boron quaternarization. The other resonance could not be detected even at high concentrations, presumably as a consequence of quadrupolar coupling in an unfavourable electric field gradient situation that leads to fast relaxation of the nuclei.³³ In ^{19}F NMR, all fluorine atoms were found to be magnetically inequivalent (Fig. S8†). We surmised that steric crowding of the bis(borane) moiety might result in hindered rotation of C_6F_5 substituents at the NMR time scale, thus differentiating the fluorine nuclei.

The crystalline materials afforded in the above-mentioned reactions could be analysed by single crystal X-ray diffraction (sc-XRD), but the obtained structures for **5** were of too poor quality to be discussed. The solid-state structures of the spectroscopically similar complexes **3** and **4** reveal that the bis(borane) moiety interacts with the terminal nitrogen *via* a single boryl centre through covalent, double B–N bonding (Fig. 3). These are the first examples of dinitrogen borylation where the BR_2 group is sourced from a triarylborane.^{34,35} The second boron atom is found as a tetraaryl borate centre, in agreement with boron NMR analysis. This $\kappa^1\text{B}$ arrangement of the bis(boron) moiety results from a C_6F_5 transfer, similar to what was observed upon methyl abstraction on $[\text{Cp}_2\text{Zr}(\text{CH}_3)_2]$ by **2** to form the anion $[\text{B}(\text{Me})(\text{C}_6\text{F}_5)(\text{C}_6\text{F}_4\{\text{B}(\text{C}_6\text{F}_5)_3\})]$,^{32c} and likely occurs as a means to mitigate steric repulsion between the C_5F_6 groups and the phosphines' substituents. The boron atoms are

essentially coplanar with the bridging C_6F_4 group, but steric tension in these edifices is revealed by the two boron centres being pushed away from each other, with C–C–B angles in the phenylene junctions approaching 130° . Meanwhile, the borate moiety significantly deviates from the ideal tetrahedral geometry. Short W–N distances (**3**: 1.788(3); **4**: 1.860(6) Å) and long N–N ones (**3**: 1.248(5); **4**: 1.249(8) Å) suggest a formal $\text{W}=\text{N}=\text{N}$ motif, and the *trans* effect from the second N_2 ligand in **4** is likely to be responsible for the elongated W–N distance compared to that of **3**. Whereas infrared spectroscopy did not allow us to clearly identify the boryldiazenido N–N bond stretches (see Fig. S1–S3 and S9, S10†), which was not surprising given the elongated N_2 unit found in **3** and **4**, resonance Raman spectroscopy of **5** shows an intense line in the spectrum at 1364 cm^{-1} (Fig. S11†). ^{15}N isotopic enrichment shifts this line to 1343 cm^{-1} (Fig. S12†). These frequencies agree with a $\text{N}=\text{N}$ linkage as they are close to those of the ν_{NN} of azo-dyes (*ca.* 1400 cm^{-1}).³⁷ A weak band observed at 2220 cm^{-1} in the IR spectrum of **4** was attributed to the terminal N_2 ligand. The bent N–N–B angles (*ca.* 140°) are typically found in other examples of boryldiazenido–tungsten complexes.^{12g,20a,b,28,33a,b,38} The B–N bonds are *ca.* 1.40 Å long, indicative of significant double B–N bonding. Collectively, these parameters point to a formal description of these compounds as $\text{W}(\text{II})$ -boryldiazenido complexes. Interestingly, the main compositional difference between **3** and **4** is also found when comparing the adducts of $\text{B}(\text{C}_6\text{F}_5)_3$ with **1^{Ph12g}** or **1^{Et12g}**: in complex **3** the *trans* coordination site features an agostic interaction involving the $\text{C}_{\text{ortho}}\text{--H}$ of a phenyl substituent of the dppe ligand, whereas the depe analogue **4** retains its second N_2 ligand. We believe that the relative instability of **3** originates from the labile agostic bond that may expose the Lewis acidic, 16-electron tungsten centre to further reactivity. Because we failed to observe double coordination of the bis(borane) to the terminal N_2 ligand of complexes **1^R**, we briefly explored the reactivity of **5** (Scheme 2). The instability of **3** in common solvents precluded such study. Among the various tests we have carried out, the reaction with dihydrogen was particularly rewarding in view of our initial goal. Treating **5** with H_2 produced almost immediately a new complex $[\text{W}(\text{H})_2(\text{depe})_2(\text{N}_2\{\text{B}(\text{C}_6\text{F}_5)_2\text{C}_6\text{F}_4\text{B}(\text{C}_6\text{F}_5)_3\})]$ (**6**) that readily decomposed upon attempting its isolation by concentration under vacuum. The ^{31}P NMR points to the occurrence of two isomers for **6**, possibly due to a hindered free rotation induced by the bulkiness of the bis(boron) moiety (Fig. S14†). Each shows four similar signals, indicative of a dissymmetry of the first coordination sphere. The ^{11}B NMR spectrum is basically unchanged. Over the course of several days, **6** evolves upon heating into a new species $[\text{W}(\text{H})_2(\text{depe})_2(\text{N}_2\{\text{B}(\text{C}_6\text{F}_5)_2\}_2\text{C}_6\text{F}_4)]$ (**7**) for which the ^{11}B NMR spectrum shows significant change in the bis(boron) moiety (disappearance of the borate signal at $\delta = -15.1$ ppm and a new, deshielded resonance at -3.4 ppm). Yellow crystals of **7** could be recovered and analysed by sc-XRD (Fig. 4), revealing oxidative addition of H_2 and the seven-coordinate nature of **7** with one isomerized depe ligand.³⁹ Remarkably, the bis(borane) pairs with the basic terminal N through two-fold single, dative-type bonding (B–N distances are *ca.* 1.61 vs. *ca.* 1.40 Å for **4**) of its two boron atoms after

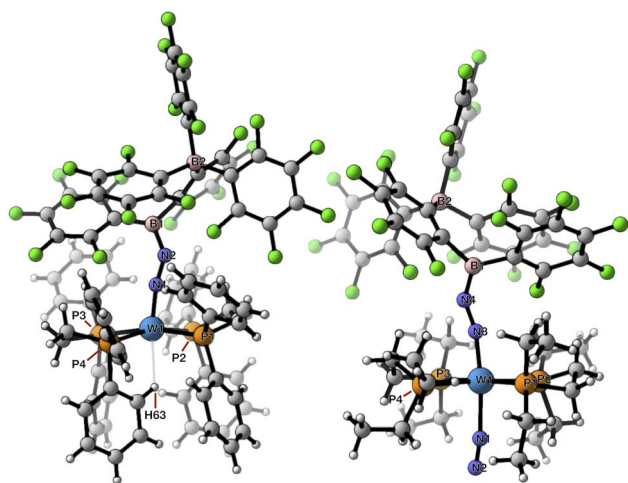
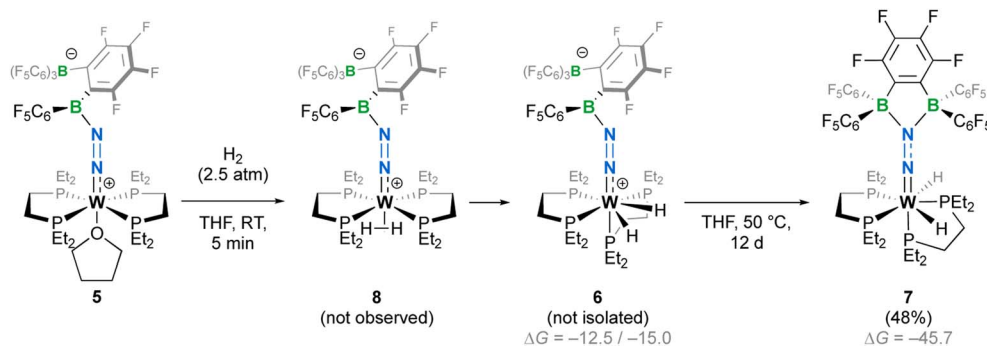


Fig. 3 Molecular structures of complexes **3** (left) and **4** (right) in the solid state rendered with CYLview20.³⁶ Selected distances (Å) and angles ($^\circ$): **3**: W1–H63 2.437, W1–N1 1.788(3), N1–N2 1.248(5), N2–B1 1.400(5), W1–N1–N2 168.9(3), N1–N2–B1 141.7(4); **4**: W1a–N1 2.155(7), N1–N2 1.117(11), W1a–N3 1.860(6), N3–N4 1.249(8), N4–B1 1.368(10), W1a–N1–N2 171.5(8), W1a–N3–N4 165.3(5), N3–N4–B1 143.9(6).





Scheme 2 Reaction of **5** with dihydrogen leading to seven-coordinate complexes **7**. Isolated yields in parentheses. ΔG (DFT, B3PW91-6-31G(d,p)) are given in kJ mol^{-1} .

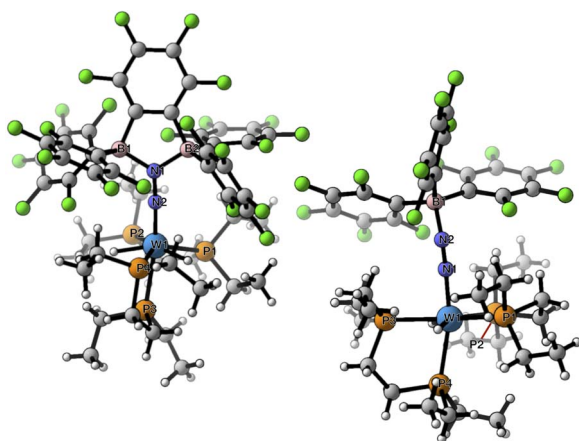


Fig. 4 Molecular structures of complexes **7** (left) and **10** (right) in the solid state. Selected distances (Å) and angles ($^\circ$): **7**: W1–P1 2.559(1), W1–P2 2.516(1), W1–P3 2.651(1), W1–P4 2.475(1), W1–N2 1.825(2), N1–N2 1.291(3), N1–B1 1.615(3), N1–B2 1.614(3), W1–H100 1.66(3), W1–H200 1.62(2), W1–N2–N1 177.0(2), N2–N1–B1 125.0(2), N2–N1–B2 121.8(2), B1–N1–B2 113.3(2). **10**: W1–P1 2.4813(5), W1–P2 2.4792(5), W1–P3 2.4300(5), W1–P4 2.5214(5), W1–N1 1.8826(17), N1–N2 1.193(2), N1–B1 1.562(3), W1–H1 1.71(3), W1–H2 1.70(3), W1–N1–N2 167.21(15), N1–N2–B1 139.13(18).

a backward C_6F_5 transfer. This results in augmented, push–pull type charge transfer to the N_2 ligand, as shown by the remarkably long N–N bond of 1.291(3) Å, going beyond that of a N–N double bond.⁴⁰ As a specific comparison, N–N bond lengths of two-fold 1,2- $\text{B}(\text{C}_6\text{F}_5)_3$ adducts of diazene (N_2H_2 , 1.230(3) Å) and diazenide (N_2H^- , 1.2227(18) Å)⁴¹ or LA adducts of diazenes (1.227(2)–1.263(4) Å) are much shorter.⁴² To the best of our knowledge, this is the first example of a neutral adduct of an end-on N_2 ligand with a ditopic Lewis acid.

DFT calculations were conducted to shed light on this transformation (see Fig. S40†). Structure optimization allowed us to locate a *trans*- $\sigma\text{-H}_2$ complex **8** and a more stable *cis*-dihydride that could well correspond to **6**. Two rotamers (**6** and **6'**) were found for the latter species, whose energy difference matches well with the experimentally observed ratio. Isomer **7** was found to be more stable than **6** by 31 kJ mol^{-1} . Estimates of ^1H chemical shifts for the W-bound protons that we were not

able to locate in the ^1H NMR spectra (see Fig. S13 and S18†) were also computed. They fall within the alkyl protons' region and probably overlap with the resonances linked to the phosphine's substituents (see Plot S1†), supporting the absence of resonances at higher fields.

The activation of dihydrogen by **5** pushed us to verify whether a simpler system, that is the adduct of $\text{B}(\text{C}_6\text{F}_5)_3$ with **1**^{Et}, *trans*- $[\text{W}(\text{N}_2)(\text{depe})_2(\text{N}_2\{\text{B}(\text{C}_6\text{F}_5)_3\})]$ (**9**), would react similarly—a positive result would also provide a comparison of the influence of a mono- vs. di-topic LA to N_2 activation. Gratifyingly, under an H_2 atmosphere, **9** evolved into the bis-hydride complex $[\text{W}(\text{H})_2(\text{depe})_2(\text{N}_2\{\text{B}(\text{C}_6\text{F}_5)_3\})]$ (**10**) without N_2 loss. We were able to isolate it in high yields and carried out its full characterization. We could not evidence FLP-type heterolytic splitting of H_2 at the B–N linkage, similar to what we observed when we reacted an adduct of **1**^{Ph} and $\text{B}(\text{C}_6\text{F}_5)_3$ with hydroboranes and -silanes.^{12g} Here, dihydrogen favoured reactivity at the reduced metal centre. sc-XRD analysis of **10** revealed a similar first coordination sphere to that of **7** (Fig. 4). The influence of dihydrogen oxidative addition on N_2 activation may be measured by comparing **10** with the adduct of $\text{B}(\text{C}_6\text{F}_5)_3$ with **1**^{Et} (**9**).^{12j} The two structures are rather similar (Table 1), with a slightly higher activation level for N_2 in **10** (1.196(2) vs. 1.179(9) Å for **9**). This is also reflected by the IR stretching frequencies (1767 cm^{-1} for **9** vs. 1712 cm^{-1} for **10**). The N–N–B angle is also more acute in **10**, which may be due to reduced steric hindrance of the isomerized first coordination sphere (Table 1). Interestingly, **7** could also be obtained from **10** in high yields by simply reacting it with one equivalent of bis(borane) **2** (Scheme 3), with $\text{B}(\text{C}_6\text{F}_5)_3$ being displaced upon slight thermal activation.

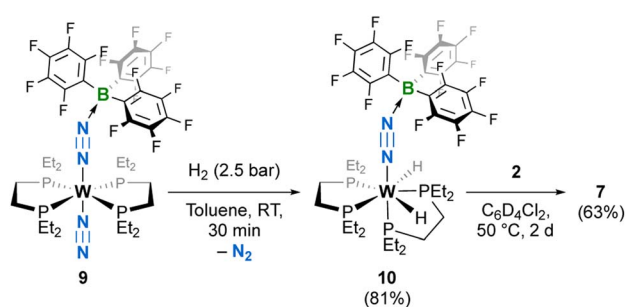
Comparison of the structures of the N_2 complexes **7** and **10** supports the depiction of the N_2 unit in **7** as a diazene-diide (N_2^{2-}) ligand (Table 1): as mentioned above, the N–N bond length (1.291(3) Å) goes beyond that of standard N–N double bonds. The linearisation of the W–N–N array in **7** (177 vs. 167 $^\circ$ for **10**) and the significant shortening of the W–N bond (1.82 vs. 1.88 Å for **10**) are also in line with the diatomic molecule being an LX-type ligand. In addition, the smaller N–N–B angles point to a fully sp^2 -hybridized distal nitrogen, as expected for the N_2^{2-} dianion.¹⁵ ^{15}N labelling of **7** and **10** allowed us to unambiguously



Table 1 Comparison of pertinent structural parameters, NN stretching frequencies. Values in parentheses were calculated by DFT (B3PW91, 6-31G(d,p), and D3BJ). Computed infrared frequencies were corrected with a scaling factor = 0.958. n.a. = not applicable. n.d. = not determined. as = asymmetric. s = symmetric

| Bonds (Å)/angles (°)/ ν (cm ⁻¹) | 1 ^{Et} | 9 ^a | 10 | 7 |
|--|----------------------------|-----------------------|-------------------|------------------------------------|
| W–N (theor.) | 2.016 | 1.908(6) | 1.883(2) (1.873) | 1.825(2) (1.831) |
| N–N (theor.) | 1.123(2) | 1.179(9); 1.08(1) | 1.193(2) (1.184) | 1.291(3) (1.243) |
| N–B (theor.) | n.a. | 1.55(1) | 1.562(3) (1.556) | 1.615(1) (1.626[0]) ^b |
| W–P _{trans} (theor.) | n.a. | n.a. | 2.5214(5) (2.512) | 2.651(1) (2.609) |
| W–N–N (theor.) | 178.6(1) | 169.0(6) | 167.2(2) (166.8) | 177.0(2) (175.9) |
| N–N–B (theor.) | n.a. | 148.4(7) | 139.1(2) (135.3) | 123.4(23) (123.6[18]) ^b |
| av. N–W–P _{eq} ^b | 90.0(9) | 91(4) | 89(4) | 99(6) |
| ν_{NN} ¹⁴ N (theor.)/ ¹⁵ N ^c | 1890/1830 (as) | 1767 | 1712 (1827)/1659 | 1399 (1548)/1338 |
| ν_{NN} ¹⁴ N/ ¹⁵ N ^d | 1968/1903 ^e (s) | n.d. | 1714/1664 | Not observed |

^a Taken from ref. 12j. ^b Averaged data; standard deviation calculated from the measurement set are not the average of the standard deviation of individual measurements. ^c FT-ATR infrared spectroscopy. ^d Resonance Raman spectroscopy. ^e Taken from ref. 43.



Scheme 3 Synthesis of bis-hydride **10** by the reaction of H₂ with the B(C₆F₅)₃ adduct of **1**^{Et}, **9**, and displacement of the borane by bis(borane) **2** to give **7**. Isolated yields in parentheses.

locate N–N stretches in their IR spectra (Table 1, Fig. S22, S23 and S31, S32†). Surprisingly, no shifting lines could be observed when comparing the Raman spectra of ¹⁴N- and ¹⁵N-**7** (Fig. S24 and S25†), while in the case of **10**, a low-intensity line at 1714 cm⁻¹ shifted to 1664 cm⁻¹ for the ¹⁵N isotopologue (Fig. S33 and S34†). The strong bathochromic shift recorded for the stretching frequency of **7** (1399 vs. 1712 cm⁻¹ for **10**) and the structural data indeed support the N=N²⁻ depiction.^{37,40–42} The reaction of **10** with **2** points to diborane coordination-triggered 2-e⁻ reduction of N₂, and somewhat recalls the evolution of the N–N bond upon the two-fold protonation of related group 6 N₂ complexes affording hydrazido complexes.²⁹ The resulting positively charged compounds show N–N bond lengths ranging from 1.30–1.37 Å depending on the *trans* ligand and H-bonding in the lattice. Interestingly, the Schrock group was, to the best of our knowledge, the only group to report structural data for both Mo-diazido and Mo-hydrazido complexes, the latter being obtained by protonation of the former. Surprisingly, the N–N bond lengths are equal for these two compounds (1.302(13) vs. 1.304(6), respectively). Although this single point of comparison prevents a general conclusion to be drawn, it is remarkable that in our case, the effect of incremental LA coordination is much more pronounced. Unfortunately, comparison of ¹⁵N NMR chemical shifts could not be performed since despite several hours of acquisition, we were not able to detect resonances for **7**

(see Fig. S7, S17 and S29† for the ¹⁵N NMR spectra of **5**, **6** and **10**, respectively).

DFT calculations including dispersion (D3BJ) were run on **7** and **10** (see the ESI for details and atomic coordinates of the computed structures). Key metrical parameters were found to be close to those experimentally determined or within the margin of error of DFT (Table 1). Comparison of the atomic charges obtained by a Natural Population Analysis (NPA) evidences that the negative charge carried by the N₂ unit in **7** (–0.46) is 1.5 times higher than that found in **10** (–0.30). In both cases, it is almost totally localized on the distal nitrogen, in agreement with previous observations,^{12f} and the N–N bond in **7** is significantly more polarised. A much higher negative charge is carried by the metal atom in **10**, in line with a diminished metal-to-N₂ charge transfer and a lower formal oxidation state attributed to its W centre. Wiberg bond indices (WBI) also reflect the trends revealed by the structures of **7** and **10**: a higher N–N WBI is found in **10** (1.94 vs. 1.57 in **7**, Fig. 5), but a lower W–N one (1.23 vs. 1.50 in **7**). As far as the B–N bonds are concerned, a smaller N–B WBI in **7** parallels the longer N–B distances found in its crystal structure (Table 1). Analysis of the Natural Bonding Orbitals (NBOs) further differentiates **7** and **10**. In **10**, the W–N bonding involves

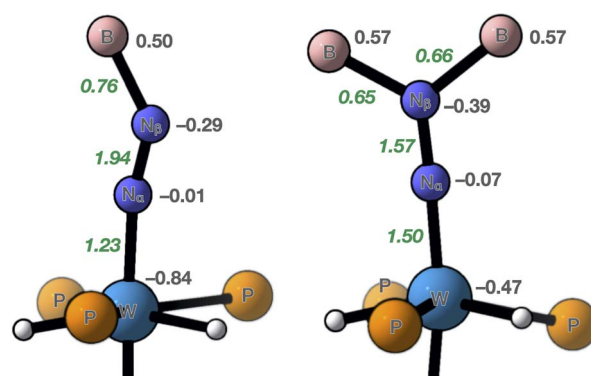


Fig. 5 Summary of key parameters from theoretical calculations run on **7** (right) and **10** (left). Grey figures are NPA charges and green italic ones, Wiberg bond indices.



mainly atomic orbitals of σ symmetry, while for **7** it is computed to rest on π -symmetric orbitals exclusively (see Fig. S51–S53† for visualization of key pNBOs and Natural Localized Molecular Orbitals [NLMOs] of **7** and **10**). In both cases, the W–N NBO is polarized towards the nitrogen atom. Interestingly, a lone pair is found on the proximal nitrogen of **7**, which undergoes significant stabilizing donor–acceptor interactions with the W–P_{trans} antibond. This is where the W–N σ -symmetric bonding lies, and this is what explains why in **7** the W–P_{trans} bond is significantly elongated compared to that of **10** (Table 1). In other terms, it translates the stronger *trans* influence of the diazene-diide ligand. Conversely, **10** carries a lone pair of pure d character on W for which second-order perturbation theory estimates an important stabilization by a donor–acceptor interaction with a π^* of N₂, thus embodying π back-donation. Moving to the N–N linkage, a single π bond is found for **7** along the σ component, whereas **10** has two, indicating an intact triple N–N linkage, unlike **7**. N–B NBOs are polarised towards nitrogen to the same extent in both compounds (*ca.* 75%), yet the natural atomic hybrids on nitrogen differ significantly from **7** to **10**, reflecting sp² and sp hybridization, respectively (see Tables S7 and S8† for a summary of pertinent values issued by NBO analysis). Collectively, these computational observations also support a 2-e[−] reduced N₂ unit, stabilised by a W(IV) centre through σ and π donation from the nitrogen ligand, as well as by two-fold dative N → B bonding in **7**.

Conclusions

We have explored the coordination of the strongly electrophilic bis(borane) **2** to terminal dinitrogen complexes [W(R₂-P(CH₂)₂PR₂)₂(N₂)₂] (**1^R**) with the hope to observe κ^2 B coordination to the distal nitrogen, thus building an orbitally adapted push–pull template for N₂ activation. The reaction with either **1^{Ph}** or **1^{Et}** did not furnish the expected outcome with formation of covalent N–B bonds in complexes *trans*-[W(L)(R₂PCH₂CH₂PR₂)₂(N₂{B(C₆F₅)₂(C₆F₄B(C₆F₅)₃})] (L = \emptyset , N₂ or THF) (**3–5**) after boron-to-boron C₆F₅ transfer. The reactivity of *trans*-[W(THF)(depe)₂(N₂{B(C₆F₅)₂C₆F₄B(C₆F₅)₃})] (**5**) with dihydrogen was then explored. It triggered backward C₆F₅ transfer upon oxidative addition of H₂, without N₂ loss, and afforded complex [W(H)₂(depe)₂(N₂{B(C₆F₅)₂C₆F₄B(C₆F₅)₃})] (**7**) having the bis(borane) coordinating the distal nitrogen *via* two-fold dative bonding. Its especially long N–N bond (1.29 Å) goes beyond reference N=N distances (1.21–1.25 Å). The B(C₆F₅)₃ analogue of **7**, complex [W(H)₂(depe)₂(N₂{B(C₆F₅)₃})] (**10**), could be prepared by oxidative addition of H₂ on adduct [W(N₂)(-depe)₂(N₂{B(C₆F₅)₃})] **9**. In **10**, B(C₆F₅)₃ can be displaced by bis(borane) **2** to furnish **7**. Comparison of **7** with **10** led us to propose that the N₂ ligand underwent 2e[−] reduction upon coordination of the bis(borane), due to an extreme push–pull effect. To the best of our knowledge, this is the first example of LA-coordination-induced reduction of an N₂ ligand, a transformation that is commonly observed upon protonation or functionalisation.^{29,30} This points to a possible strong influence of the multiple H-bonding channel when N₂ is coordinated to

the FeMo cofactor of the nitrogenases. Guidelines for future N₂ fixation FLP systems may also be drawn from our study as we demonstrate that bis(borane) can trigger reduction of the diatomic molecule when combined to an electron-rich species, a reactivity commonly observed in small molecule activation by FLPs. Future work will focus on the reactivity of **7** and **10**, new complexes that have the rare but remarkable ability to activate N₂ and H₂ at a single metal centre;^{22d,44} promoting N–H bond formation in such species should be facilitated by the proximity of the two hydrides with the N₂ ligand.⁴⁵

Data availability

All the relevant curated data can be found in the ESI† as stated in the footnote. Raw data were not uploaded into repositories.

Author contributions

D. S., M.-C. B., A. C. and L. E. run the experiments and analyzed the data. L. V. recorded single-crystal X-ray diffraction data and solved the structures. M. G. performed DFT calculations and assisted in the writing of the manuscript. A. S. obtained funding for the project and managed it, conceived the original idea, designed the experiments and took part in the analysis of the data. D. S. wrote the preliminary manuscript draft and A. S. took charge of writing the submitted and revised versions. D. S., M.-C. B., M. G. and A. S. were involved in the writing of the ESI.† All authors were involved in the proof-reading process.

Conflicts of interest

There are no conflicts to declare.

Acknowledgements

The authors would like to thank Pr. François P. Gabbaï, Dr Mitsukimi Tsunoda and Dr Kirill I. Tugashov for providing expert advice on the synthesis of [HgC₆F₄]₃ necessary to prepare bis(borane) **2**. D. S., M.-C. B. and A. S. are indebted to the European Research Council for funding (ERC Starting Grant no 757501). A. C. is grateful to the French Ministry of National and Superior Education and Research (MENESR) for a PhD fellowship. This work was partly supported by the ANR PUNCH project (post-doc fellowship for L. E.), grant ANR-21-CE07-0003 of the French Agence Nationale de la Recherche.

References

- (a) F. Masero, M. A. Perrin, S. Dey and V. Mougél, *Chem.–Eur. J.*, 2021, **27**, 3892–3928; (b) D. Singh, W. R. Buratto, J. F. Torres and L. J. Murray, *Chem. Rev.*, 2020, **120**, 5517–5581; (c) *Transition Metal-Dinitrogen Complexes: Preparation and Reactivity*, ed. Y. Nishibayashi, Wiley-VCH Verlag GmbH & Co. KGaA, Weinheim, Germany, 2019; (d) R. J. Burford and M. D. Fryzuk, *Nat. Rev. Chem.*, 2017, **1**, 1–13; (e) M. D. Walter, in *Advances in Organometallic Chemistry*, ed. P. J. Pérez, Elsevier, 2016, vol. 65, pp. 261–377.



- 2 (a) Y. Tanabe, in *Transition Metal-Dinitrogen Complexes*, 2019; (b) Z. R. Turner, *Inorganics*, 2015, **3**, 597–635; (c) M. G. Gardiner and D. N. Stringer, *Materials*, 2010, **3**, 841–862; (d) W. J. Evans and D. S. Lee, *Can. J. Chem.*, 2005, **83**, 375–384.
- 3 (a) B. Rösch, T. X. Gentner, J. Langer, C. Färber, J. Eyselein, L. Zhao, C. Ding, G. Frenking and S. Harder, *Science*, 2021, **371**, 1125–1128; (b) R. Mondal, K. Yuvaraj, T. Rajeshkumar, L. Maron and C. Jones, *Chem. Commun.*, 2022, **58**, 12665–12668.
- 4 (a) M.-A. Légaré, G. Bélanger-Chabot, R. D. Dewhurst, E. Welz, I. Krummenacher, B. Engels and H. Braunschweig, *Science*, 2018, **359**, 896–900; (b) M.-A. Légaré, M. Rang, G. Bélanger-Chabot, J. I. Schweizer, I. Krummenacher, R. Bertermann, M. Arrowsmith, M. C. Holthausen and H. Braunschweig, *Science*, 2019, **363**, 1329–1332; (c) M.-A. Légaré, G. Bélanger-Chabot, M. Rang, R. D. Dewhurst, I. Krummenacher, R. Bertermann and H. Braunschweig, *Nat. Chem.*, 2020, **12**, 1076–1080; (d) S. Bennaamane, B. Rialland, L. Khrouz, M. Fustier-Boutignon, C. Bucher, E. Clot and N. Mézailles, *Angew. Chem., Int. Ed.*, 2023, **62**, e202209102.
- 5 (a) Y. Tanabe and Y. Nishibayashi, *Chem. Soc. Rev.*, 2021, **50**, 5201–5242; (b) Q. J. Bruch, G. P. Connor, N. D. McMillion, A. S. Goldman, F. Hasanayn, P. L. Holland and A. J. M. Miller, *ACS Catal.*, 2020, **10**, 10826–10846; (c) M. J. Chalkley, M. W. Drover and J. C. Peters, *Chem. Rev.*, 2020, **120**, 5582–5636; (d) S. L. Foster, S. I. P. Bakovic, R. D. Duda, S. Maheshwari, R. D. Milton, S. D. Minter, M. J. Janik, J. N. Renner and L. F. Greenlee, *Nat. Catal.*, 2018, **1**, 490–500; (e) N. Stucke, B. M. Flöser, T. Weyrich and F. Tuczek, *Eur. J. Inorg. Chem.*, 2018, **2018**, 1337–1355; (f) *Nitrogen Fixation*, ed. Y. Nishibayashi, Springer International Publishing AG, Cham, Switzerland, 2017; (g) Y. Roux, C. Duboc and M. Gennari, *ChemPhysChem*, 2017, **18**, 2606–2617.
- 6 (a) M. Appl, *Ammonia, 2. Production Processes*, 2011; (b) G. Ertl, *Angew. Chem., Int. Ed.*, 2008, **47**, 3524–3535; (c) J. W. Erisman, M. A. Sutton, J. Galloway, Z. Klimont and W. Winiwarter, *Nat. Geosci.*, 2008, **1**, 636; (d) R. Schlögl, *Angew. Chem., Int. Ed.*, 2003, **42**, 2004–2008; (e) V. Smil, *Enriching the Earth: Fritz Haber, Carl Bosch, and the Transformation of World Food Production*, Mit Press, 2001; (f) V. Smil, *Nature*, 1999, **400**, 415; (g) J. R. Jennings, *Catalytic Ammonia Synthesis: Fundamentals and Practice*, Springer, New York, 1991.
- 7 (a) S. Kim, F. Loose and P. J. Chirik, *Chem. Rev.*, 2020, **120**, 5637–5681; (b) Z.-J. Lv, J. Wei, W.-X. Zhang, P. Chen, D. Deng, Z.-J. Shi and Z. Xi, *Natl. Sci. Rev.*, 2020, **7**, 1564–1583.
- 8 (a) O. Einsle and D. C. Rees, *Chem. Rev.*, 2020, **120**, 4969–5004; (b) L. C. Seefeldt, Z.-Y. Yang, D. A. Lukoyanov, D. F. Harris, D. R. Dean, S. Raugei and B. M. Hoffman, *Chem. Rev.*, 2020, **120**, 5082–5106; (c) B. M. Hoffman, D. Lukoyanov, Z.-Y. Yang, D. R. Dean and L. C. Seefeldt, *Chem. Rev.*, 2014, **114**, 4041–4062; (d) K. Tanifuji and Y. Ohki, *Chem. Rev.*, 2020, **120**, 5194–5251.
- 9 D. Dubois and R. Hoffmann, *Nouv. J. Chim.*, 1977, **1**, 479–492.
- 10 S. Gambarotta and J. Scott, *Angew. Chem., Int. Ed.*, 2004, **43**, 5298–5308.
- 11 (a) A. Coffinet, A. Simonneau and D. Specklin, in *Encyclopedia of Inorganic and Bioinorganic Chemistry*, ed. R. A. Scott, Wiley-VCH Verlag GmbH & Co. KGaA, 2020, pp. 1–25; (b) A. J. Ruddy, D. M. C. Ould, P. D. Newman and R. L. Melen, *Dalton Trans.*, 2018, **47**, 10377–10381; (c) A. Simonneau and M. Etienne, *Chem.-Eur. J.*, 2018, **24**, 12458–12463.
- 12 (a) J. Chatt, J. R. Dilworth, R. L. Richards and J. R. Sanders, *Nature*, 1969, **224**, 1201–1202; (b) J. Chatt, R. H. Crabtree and R. L. Richards, *J. Chem. Soc. Chem. Commun.*, 1972, 534; (c) J. Chatt, R. H. Crabtree, E. A. Jeffery and R. L. Richards, *J. Chem. Soc. Dalton Trans.*, 1973, 1167–1172; (d) F. Studt, B. A. MacKay, S. A. Johnson, B. O. Patrick, M. D. Fryzuk and F. Tuczek, *Chem.-Eur. J.*, 2005, **11**, 604–618; (e) H. Broda, S. Hinrichsen, J. Krahmer, C. Nather and F. Tuczek, *Dalton Trans.*, 2014, **43**, 2007–2012; (f) J. B. Geri, J. P. Shanahan and N. K. Szymczak, *J. Am. Chem. Soc.*, 2017, **139**, 5952–5956; (g) A. Simonneau, R. Turrel, L. Vendier and M. Etienne, *Angew. Chem., Int. Ed.*, 2017, **56**, 12268–12272; (h) L. G. Pap, A. Couldridge, N. Arulsamy and E. Hulley, *Dalton Trans.*, 2019, **48**, 11004–11017; (i) J. P. Shanahan and N. K. Szymczak, *J. Am. Chem. Soc.*, 2019, **141**, 8550–8556; (j) D. Specklin, A. Coffinet, L. Vendier, I. del Rosal, C. Dinoi and A. Simonneau, *Inorg. Chem.*, 2021, **60**, 5545–5562.
- 13 (a) P. C. Dos Santos, R. Y. Igarashi, H.-I. Lee, B. M. Hoffman, L. C. Seefeldt and D. R. Dean, *Acc. Chem. Res.*, 2005, **38**, 208–214; (b) T. Spatzal, K. A. Perez, O. Einsle, J. B. Howard and D. C. Rees, *Science*, 2014, **345**, 1620–1623; (c) S. M. Keable, J. Vertemara, O. A. Zadornyy, B. J. Eilers, K. Danyal, A. J. Rasmussen, L. De Gioia, G. Zampella, L. C. Seefeldt and J. W. Peters, *J. Inorg. Biochem.*, 2018, **180**, 129–134; (d) D. Sippel, M. Rohde, J. Netzer, C. Trncik, J. Gies, K. Grunau, I. Djurdjevic, L. Decamps, S. L. A. Andrade and O. Einsle, *Science*, 2018, **359**, 1484–1489; (e) W. Kang, C. C. Lee, A. J. Jasiewski, M. W. Ribbe and Y. Hu, *Science*, 2020, **368**, 1381–1385. Although the structural data reported in this latter reference have been the matter of a discussion, the role of acidic residues in the nitrogenases' active site for N₂ activation remains a solid hypothesis, see ref. 8a–c and 13a.(f) J. W. Peters, O. Einsle, D. R. Dean, S. DeBeer, B. M. Hoffman, P. L. Holland and L. C. Seefeldt, *Science*, 2021, **371**, eabe5481; (g) K. Wonchull, C. C. Lee, A. J. Jasiewski, M. W. Ribbe and Y. Hu, *Science*, 2021, **371**, eabe5856.
- 14 This has pushed several groups to explore the influence of inter- or intramolecular acidic or basic functions to mimic secondary-sphere interactions: (a) P. Bhattacharya, D. E. Prokopchuk and M. T. Mock, *Coord. Chem. Rev.*, 2017, **334**, 67–83; (b) S. E. Creutz and J. C. Peters, *Chem. Sci.*, 2017, **8**, 2321–2328.
- 15 (a) J. C. Slootweg and A. R. Jupp, *Frustrated Lewis Pairs*, Springer Nature, 2020; (b) D. W. Stephan, *Science*, 2016, **354**, aaf7229; (c) D. W. Stephan, *Acc. Chem. Res.*, 2015, **48**,



- 306–316; (d) D. W. Stephan and G. Erker, *Angew. Chem., Int. Ed.*, 2015, **54**, 6400–6441; (e) *Frustrated Lewis Pairs I: Uncovering and Understanding*, ed. G. Erker and D. W. Stephan, Springer Berlin Heidelberg, 2013; (f) *Frustrated Lewis Pairs II: Expanding the Scope*, ed. G. Erker and D. W. Stephan, Springer Berlin Heidelberg, 2013; (g) D. W. Stephan and G. Erker, *Angew. Chem., Int. Ed.*, 2010, **49**, 46–76.
- 16 Zhu and colleagues proposed a series of *in silico* models, see: (a) J. Zhu, *Chem.-Asian J.*, 2019, **14**, 1413–1417; (b) A. M. Rouf, Y. Huang, S. Dong and J. Zhu, *Inorg. Chem.*, 2021, **60**, 5598–5606; (c) C. Dai, Y. Huang and J. Zhu, *Organometallics*, 2022, **41**, 1480–1487; (d) J. Zeng, R. Qiu and J. Zhu, *Chem.-Asian J.*, 2023, **18**, e202201236.
- 17 R. L. Melen, *Angew. Chem., Int. Ed.*, 2018, **57**, 880–882.
- 18 C. Tang, Q. Liang, A. R. Jupp, T. C. Johnstone, R. C. Neu, D. Song, S. Grimme and D. W. Stephan, *Angew. Chem., Int. Ed.*, 2017, **56**, 16588–16592.
- 19 L. L. Cao, J. Zhou, Z.-W. Qu and D. W. Stephan, *Angew. Chem., Int. Ed.*, 2019, **58**, 18487–18491.
- 20 (a) A. Coffinet, D. Specklin, L. Vendier, M. Etienne and A. Simonneau, *Chem.-Eur. J.*, 2019, **25**, 14300–14303; (b) A. Coffinet, D. Zhang, L. Vendier, S. Bontemps and A. Simonneau, *Dalton Trans.*, 2021, **50**, 5582–5589; (c) A. Coffinet, D. Specklin, Q. Le Dé, S. Bennaamane, L. Muñoz, L. Vendier, E. Clot, N. Mézailles and A. Simonneau, *Chem.-Eur. J.*, 2023, **29**, e202203774.
- 21 (a) C. Sivasankar, P. K. Madarasi and M. Tamizmani, *Eur. J. Inorg. Chem.*, 2020, 1383–1395; (b) M. Hölscher and W. Leitner, *Chem.-Eur. J.*, 2017, **23**, 11992–12003.
- 22 Selected examples: (a) A. Sacco and M. Rossi, *Inorg. Chim. Acta*, 1968, **2**, 127–132; (b) L. J. Archer and T. A. George, *Inorg. Chem.*, 1979, **18**, 2079–2082; (c) D. G. H. Hetterscheid, B. S. Hanna and R. R. Schrock, *Inorg. Chem.*, 2009, **48**, 8569–8577; (d) H. Fong, M.-E. Moret, Y. Lee and J. C. Peters, *Organometallics*, 2013, **32**, 3053–3062.
- 23 G. C. Welch and D. W. Stephan, *J. Am. Chem. Soc.*, 2007, **129**, 1880–1881.
- 24 (a) M. Tamizmani and C. Sivasankar, *Eur. J. Inorg. Chem.*, 2017, **2017**, 4239–4245; (b) L. R. Doyle, A. J. Woolees and S. T. Liddle, *Angew. Chem., Int. Ed.*, 2019, **58**, 6674–6677.
- 25 Uranium nitride was shown to be hydrogenated in the presence of borane *via* an FLP-related mechanism: L. Chatelain, E. Louyriac, I. Douair, E. Lu, F. Tuna, A. J. Woolees, B. M. Gardner, L. Maron and S. T. Liddle, *Nat. Commun.*, 2020, **11**, 337.
- 26 F. F. Martins and V. Krewald, *Eur. J. Inorg. Chem.*, 2023, e202300268.
- 27 A bis(borane) adduct of a side-on Sm–N₂ complex was reported recently. However, it is not clear whether the reduction of dinitrogen in this complex is the result of bis(borane) coordination *via* a push–pull mechanism, or occurs through capture by Sm prior to interaction with bis(borane). S. Xu, L. A. Essex, J. Q. Nguyen, P. Farias, J. W. Ziller, W. H. Harman and W. J. Evans, *Dalton Trans.*, 2021, **50**, 15000–15002.
- 28 Diborane(4) compound B₂Br₄(SMe₂)₂ has also been explored for N₂ functionalisation and furnishes boranylboroyldiazenido complexes: L. C. Haufe, M. Arrowsmith, M. Dietz, A. Gärtner, R. Bertermann and H. Braunschweig, *Dalton Trans.*, 2022, **51**, 12786–12790.
- 29 Selected examples of structurally characterized group 6 hydrazido complexes: (a) G. A. Heath, R. Mason and K. M. Thomas, *J. Am. Chem. Soc.*, 1974, **96**, 259–260; (b) M. Hidai, T. Kodama, M. Sato, M. Harakawa and Y. Uchida, *Inorg. Chem.*, 1976, **15**, 2694–2697; (c) J. E. Barclay, A. Hills, D. L. Hughes, G. J. Leigh, C. J. Macdonald, M. A. Bakar and H. Mohd.-Ali, *J. Chem. Soc., Dalton Trans.*, 1990, 2503–2507; (d) D. V. Yandulov and R. R. Schrock, *Inorg. Chem.*, 2005, **44**, 1103–1117; (e) K. Arashiba, Y. Miyake and Y. Nishibayashi, *Nat. Chem.*, 2011, **3**, 120–125.
- 30 For two-fold N_β covalent functionalisation with main group electrophiles, see: (a) H. Oshita, Y. Mizobe and M. Hidai, *Chem. Lett.*, 1990, 1303–1306; (b) H. Oshita, Y. Mizobe and M. Hidai, *Organometallics*, 1992, **11**, 4116–4123; (c) H. Oshita, Y. Mizobe and M. Hidai, *J. Organomet. Chem.*, 1993, **456**, 213–220; (d) M.-E. Moret and J. C. Peters, *J. Am. Chem. Soc.*, 2011, **133**, 18118–18121; (e) P. A. Rudd, N. Planas, E. Bill, L. Gagliardi and C. C. Lu, *Eur. J. Inorg. Chem.*, 2013, **2013**, 3898–3906; (f) D. L. M. Suess and J. C. Peters, *J. Am. Chem. Soc.*, 2013, **135**, 4938–4941; (g) Q. Liao, N. Saffon-Merceron and N. Mézailles, *Angew. Chem., Int. Ed.*, 2014, **53**, 14206–14210; (h) Q. Liao, N. Saffon-Merceron and N. Mézailles, *ACS Catal.*, 2015, **5**, 6902–6906.
- 31 L. Greb, *Chem.-Eur. J.*, 2018, **24**, 17881–17896.
- 32 (a) V. C. Williams, W. E. Piers, W. Clegg, M. R. J. Elsegood, S. Collins and T. B. Marder, *J. Am. Chem. Soc.*, 1999, **121**, 3244–3245; (b) P. A. Chase, L. D. Henderson, W. E. Piers, M. Parvez, W. Clegg and M. R. J. Elsegood, *Organometallics*, 2006, **25**, 349–357; (c) V. C. Williams, C. Dai, Z. Li, S. Collins, W. E. Piers, W. Clegg, M. R. J. Elsegood and T. B. Marder, *Angew. Chem., Int. Ed.*, 1999, **38**, 3695–3698; (d) S. P. Lewis, N. J. Taylor, W. E. Piers and S. Collins, *J. Am. Chem. Soc.*, 2003, **125**, 14686–14687; (e) S. P. Lewis, L. D. Henderson, B. D. Chandler, M. Parvez, W. E. Piers and S. Collins, *J. Am. Chem. Soc.*, 2005, **127**, 46–47; (f) S. P. Lewis, J. Chai, S. Collins, T. J. J. Sciarone, L. D. Henderson, C. Fan, M. Parvez and W. E. Piers, *Organometallics*, 2009, **28**, 249–263.
- 33 For related compounds whose ¹¹B resonances could not be detected, see ref. 12g, 20a, 20b, 28 and (a) A. Rempel, S. K. Møllerup, F. Fantuzzi, A. Herzog, A. Deifßenberger, R. Bertermann, B. Engels and H. Braunschweig, *Chem.-Eur. J.*, 2020, **26**, 16019–16027; (b) A. Bouammali, A. Coffinet, L. Vendier and A. Simonneau, *Dalton Trans.*, 2022, **51**, 10697–10701. Other unrelated diamagnetic boron species that are NMR silent can be found in: (c) J. M. Farrell and D. W. Stephan, *Angew. Chem., Int. Ed.*, 2015, **54**, 5214–5217; (d) L. Zhu and R. Kinjo, *Angew. Chem., Int. Ed.*, 2023, **62**, e202306519.



- 34 A N₂-derived titanium nitride was shown to undergo similar N-borylation through C₆F₅ group transfer: Z. Mo, T. Shima and Z. Hou, *Angew. Chem., Int. Ed.*, 2020, **59**, 8635–8644.
- 35 For a review on N₂ borylation, see: A. Simonneau, *New J. Chem.*, 2021, **45**, 9294–9301.
- 36 C. Y. Legault, *CYLview20*, <http://www.cylview.org> 2020.
- 37 A. V. Zemskov, G. N. Rodionova, Yu. G. Tuchin and V. V. Karpov, *J. Appl. Spectrosc.*, 1988, **49**, 1020–1024.
- 38 H. Ishino, Y. Ishii and M. Hidai, *Chem. Lett.*, 1998, **27**, 677–678.
- 39 Related bis-diphosphine group 6 NO complexes were shown to activate H₂ with the same first sphere isomerisation: A. Dybov, O. Blacque and H. Berke, *Eur. J. Inorg. Chem.*, 2010, 3328–3337.
- 40 P. Pyykkö and M. Atsumi, *Chem.–Eur. J.*, 2009, **15**, 12770–12779.
- 41 Z. Hussain, Y. Luo, Y. Wu, Z. Qu, S. Grimme and D. W. Stephan, *J. Am. Chem. Soc.*, 2023, **145**, 7101–7106.
- 42 F. Reiß, A. Schulz and A. Villinger, *Chem.–Eur. J.*, 2014, **20**, 11800–11811.
- 43 F. Tuczek, K. H. Horn and N. Lehnert, *Coord. Chem. Rev.*, 2003, **245**, 107–120.
- 44 (a) W. H. Bernskoetter, E. Lobkovsky and P. J. Chirik, *Organometallics*, 2005, **24**, 6250–6259; (b) R. P. Yu, J. M. Darmon, S. P. Semproni, Z. R. Turner and P. J. Chirik, *Organometallics*, 2017, **36**, 4341–4343; (c) S. M. Rummelt, H. Zhong, N. G. Léonard, S. P. Semproni and P. J. Chirik, *Organometallics*, 2019, **38**, 1081–1090.
- 45 M. M. Deegan and J. C. Peters, *Chem. Sci.*, 2018, **9**, 6264–6270.

